

## Optical properties of $\text{MgNb}_2\text{O}_6$ single crystals: a comparison with $\text{LiNbO}_3$

This article has been downloaded from IOPscience. Please scroll down to see the full text article.

1995 J. Phys.: Condens. Matter 7 2249

(<http://iopscience.iop.org/0953-8984/7/11/002>)

View [the table of contents for this issue](#), or go to the [journal homepage](#) for more

Download details:

IP Address: 171.66.16.179

The article was downloaded on 13/05/2010 at 12:45

Please note that [terms and conditions apply](#).

## Optical properties of $\text{MgNb}_2\text{O}_6$ single crystals: a comparison with $\text{LiNbO}_3$

C Zaldo†, M J Martín†, C Coya†, K Polgár‡, A Péter‡ and J Paitz§

† Instituto de Ciencia de Materiales de Madrid, Consejo Superior de Investigaciones Científicas, Campus Universitario de Cantoblanco C-IV, 28049 Madrid, Spain

‡ Research Laboratory for Crystal Physics, Hungarian Academy of Sciences, PO Box 132, 1502 Budapest, Hungary

§ Central Research Institute for Physics, Hungarian Academy of Sciences, PO Box 49, H1525 Budapest 114, Hungary

Received 22 July 1994, in final form 19 December 1994

**Abstract.** As-grown  $\text{MgNb}_2\text{O}_6$  single crystals grown by the Czochralski method show a deep-blue colour due to the presence of broad optical absorption in the visible spectral region. The absorption of the samples is modified by thermal treatments in air and in vacuum. By heating in air the samples become transparent and by heating in a  $1 \times 10^{-2}$  mbar vacuum a complex and broad absorption is induced. An energy band gap of  $5.25 \pm 0.15$  eV has been determined. Oxidized samples have an absorption edge at 4.20 eV (at 15 K) but some pre-edge absorption is also present. This latter absorption and the associated photoluminescence emission with a maximum at 2.5 eV are attributed to interstitial Nb ions or Nb ions in Mg lattice sites. The optical absorptions induced by x-ray irradiation and vacuum reduction have been discussed in terms of the defects introduced. An absorption band at 2.30 eV induced by x-ray irradiation is attributed to holes trapped in oxygen ( $\text{O}^-$ -bound small polarons). The absorption band at 1.69 eV has been attributed to an electron trapped in  $\text{Nb}^{5+}$  ions ( $\text{Nb}^{4+}$  small polarons). Another absorption observed at 1.20 eV has been ascribed to a Mg-related electron trap centre. The possible presence of bipolaron centres and other electronic traps is discussed. A comparison with the optical absorption bands observed in  $\text{LiNbO}_3$  crystals has been established.

### 1. Introduction

Some ferroelectric niobate single crystals have found widespread application as optoelectronic materials because of the high value of their irreversible optical damage threshold and good electro-optic, nonlinear optic and acousto-optic properties.  $\text{LiNbO}_3$  single crystals are preferred as a substrate for waveguide fabrication [1] and have been used as a model material to demonstrate optical devices including pioneering work on the photorefractive effect [2]. Other niobates such as  $\text{KNbO}_3$  or  $\text{Sr}_x\text{Ba}_{1-x}\text{Nb}_2\text{O}_6$  also show interesting optoelectronic properties.

Most of the studies performed up to now about defects in niobate crystals concern  $\text{LiNbO}_3$ . The state of the art in the latter material has been reviewed recently [3].  $\text{LiNbO}_3$  is a non-stoichiometric material and the optical properties observed depend on intrinsic defects associated with the lack of stoichiometry [4] and crystal growth procedure. The nature of these defects is not fully understood.

For instance, to explain the coloration induced in congruent  $\text{LiNbO}_3$  by thermal annealing in vacuum (thermal reduction), some workers assume the migration of Li and Nb ions remaining after the oxygen loss to pre-existing lattice defects (a Nb vacancy associated

with an antisited niobium) [3] while others assume the creation of oxygen vacancies [5, 6]. The process is further complicated by the Li out-diffusion during heating [7] which is not recovered by oxidation in air.

Colouration has also been observed in  $\text{LiNbO}_3$  when defects are created by x-ray [8] or by high-energy electron [9] irradiation.

Unfortunately there is little information about the defect-related optical absorption properties of niobates other than  $\text{LiNbO}_3$ . The availability of this information may help in the understanding of the defects present in  $\text{LiNbO}_3$  and the optical features associated with them.

Niobium and magnesium ions in  $\text{MgNb}_2\text{O}_6$  single crystals have an oxygen coordination similar to that observed in  $\text{LiNbO}_3$  while the stacking of cations is different. A plot of the structure can be found in [10]. In  $\text{MgNb}_2\text{O}_6$ , niobium and magnesium are piled up along the *c* axis in separate chains. This means that every niobium is linked to two other niobium neighbours; thus the presence of defects related to isolated niobium ions and to niobium pairs may be expected in a high concentration. This situation is different from the case of  $\text{LiNbO}_3$  where the concentration of niobium pairs is limited to the antisited niobium atoms (5.9% in congruent  $\text{LiNbO}_3$ ) [11].

Furthermore mixed magnesium–niobium oxides (namely,  $\text{Mg}_4\text{Nb}_2\text{O}_9$  and other undetermined phases) are formed when thin layers of  $\text{KNbO}_3$  are deposited at high temperature on  $\text{MgO}$  [12]. Thus magnesium–niobium oxides may influence the optical properties and refractive index distribution of waveguides created by this method and very little is known about their optical properties.

The purpose of this work is to characterize the optical properties of  $\text{MgNb}_2\text{O}_6$  single crystals and to discuss the optical features in common with those observed in  $\text{LiNbO}_3$ .

## 2. Experimental techniques

$\text{MgNb}_2\text{O}_6$  single crystals were grown by the Czochralski technique and was pulled from a melt at 1620 °C. Johnson Matthey (grade A)  $\text{MgO}$  and  $\text{Nb}_2\text{O}_5$  powders were melted in an iridium crucible. The growth was carried out in a  $\text{N}_2$  atmosphere enriched with 2% oxygen. More details of the crystal growth procedure have been reported elsewhere [13]. After oxidation (see section 3.1) the samples appear free of inclusions and have good optical quality.

An iridium molar concentration in the crystal of 4150 ppm was determined by ionically coupled plasma spectroscopy. For this purpose,  $\text{MgNb}_2\text{O}_6$  samples were fused with  $\text{K}_2\text{S}_2\text{O}_8$ .

The crystal boule was oriented by the x-ray diffraction technique and oriented plates were sawn and polished to optical quality.

Optical absorption measurements were performed with a Varian spectrophotometer (model Cary 17). The spectral range of operation covers the 200–2500 nm region. Photoluminescence measurements were taken with a Jobin–Yvon spectrofluorometer (model JY305). In both cases a closed-cycle He-gas Lake Shore-CTi cryostat was used to cool the samples in the 15–300 K temperature range.

The samples were irradiated at 15 K with polychromatic x-rays emitted by a Siemens x-ray generator (model Kristalloflex 2H) with a tungsten anode and a beryllium window. The low-energy x-rays emitted were filtered with a 2 mm aluminium plate. The x-ray source was operated at 40 kV and 30 mA. The sample was held 6 cm away from the output x-ray window. Under these experimental conditions the irradiation sample dose is estimated to be about  $0.5 \text{ krad min}^{-1}$ .

Thermal reduction treatments were performed in a sealed ceramic tube evacuated to pressures lower than  $2 \times 10^{-2}$  mbar, while oxidizing treatments were performed at atmospheric pressure in air. In both cases the sample was kept in a platinum box and heated in a conventional furnace.

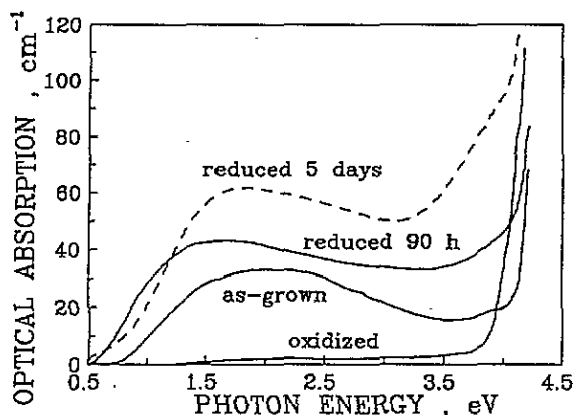


Figure 1. Room-temperature optical absorption of  $MgNb_2O_6$  single crystals in their as-grown state, after oxidation annealing in air for 7 d at  $950^\circ C$ , after reduction for 90 h in vacuum ( $10^{-3}$  mbar) at  $950^\circ C$  and after reduction for 5 d in vacuum ( $10^{-2}$  mbar) at  $970^\circ C$  (---).

### 3. Experimental results

#### 3.1. Optical properties of as-grown and oxidized samples

As-grown crystals have a deep-blue colour which is stable at room temperature. Figure 1 shows the optical absorption of the as-grown samples measured at room temperature. A broad absorption with a maximum at 2 eV is observed in the spectrum.

The absorption observed in as-grown crystals is removed by heating the samples in air at a high temperature (above  $850^\circ C$ ). Figure 1 includes the spectrum measured after heating for 7 d in air at  $950^\circ C$ . Hereafter we shall refer to this state as oxidized. It is worth noting that the oxidation annealing also induces a shift in the increasing absorption close to the band gap. As shown in the next paragraph, this shift hides the true absorption associated with the band-to-band transition when the optical absorption coefficient is lower than about  $350 \text{ cm}^{-1}$ .

In order to determine the band-gap energy  $E_0$  and optical absorption edge of  $MgNb_2O_6$  crystals, the optical absorption of a thin oxidized sample ( $78 \mu\text{m}$  thick) was recorded at several temperatures  $T$  below 300 K. Figure 2 shows a logarithmic plot of the optical absorption coefficient  $\alpha$  in the spectral region close to the absorption band gap. At a sufficiently high photon energy  $E$ , a linear dependence of  $\ln \alpha$  versus the photon energy is observed. This is expected from an Urbach-rule-type dependence [14]. Moreover a pre-edge absorption which does not follow the linear dependence is also clearly observed. The analysis of the linear regimes with the Urbach expression  $\alpha = \alpha_0 \exp[-\sigma(E_0 - E)/kT]$ ,  $k$  being the Boltzmann constant, yields a band-gap energy  $E_0 = 5.25 \pm 0.15 \text{ eV}$ .

The optical absorption edge defined phenomenologically as the photon energy where  $\ln \alpha = 4.605$  ( $\alpha = 100 \text{ cm}^{-1}$ ), has been calculated from extrapolation of the linear part of the curves shown in figure 2. The results as a function of the temperature are summarized in the inset of figure 2.

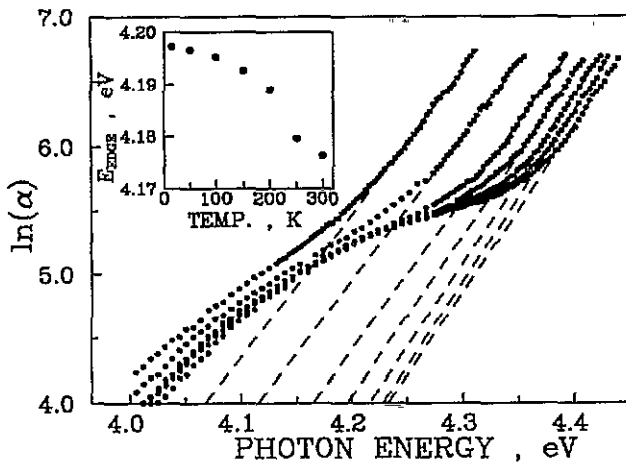


Figure 2. Optical absorption of a thin (78  $\mu\text{m}$ )  $\text{MgNb}_2\text{O}_6$  oxidized single crystal measured at several cryogenic temperatures. From right to left, the temperatures of measurement were 15, 50, 100, 150, 200, 250 and 298 K. The inset shows the photon energies for which the extrapolated linear absorption regimes (---) are  $100 \text{ cm}^{-1}$ .

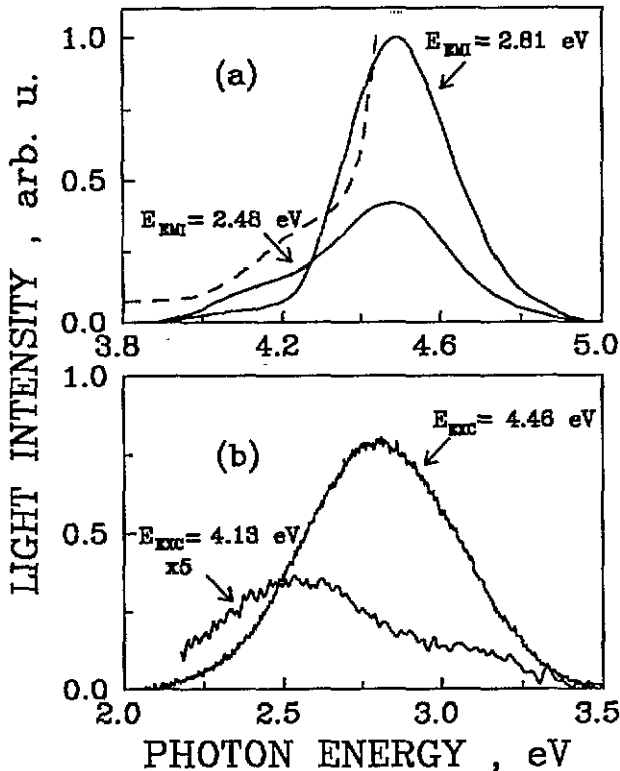


Figure 3. Photoluminescence of  $\text{MgNb}_2\text{O}_6$  oxidized single crystals measured at 15 K.  $E_{\text{EMI}}$  and  $E_{\text{EXC}}$  are the emission and excitation energies, respectively. (a) Excitation spectra: The optical absorption at 15 K is given for reference (---). (b) Emission spectra.

Figure 3 shows the photoluminescence of oxidized  $\text{MgNb}_2\text{O}_6$  crystals excited at 15 K with ultraviolet light. Figure 3(a) shows the excitation spectra and figure 3(b) shows the emission spectra. On excitation at 4.46 eV and thus above the absorption edge corresponding to 15 K, the emission is centred at 2.8 eV. This result is in agreement with previous photoluminescence measurements performed on  $\text{MgNb}_2\text{O}_6$  ceramics [15]. Moreover a weaker emission with a maximum at 2.5 eV is observed when the energy of the excitation

light is below the absorption edge. It is worth noting that the shoulder observed in the excitation spectrum of the latter emission has a spectral distribution similar to that observed in figure 3(a) for the pre-edge absorption.

### 3.2. X-ray-induced optical absorption in oxidized $MgNb_2O_6$

An oxidized sample showing only a weak optical absorption in the visible has been irradiated with x-rays at 15 K. The residual optical absorption before the irradiation is shown in figure 4 (dashed curve). After x-ray irradiation a broad absorption covering from 0.5 eV up to the absorption edge is observed. This absorption decreases upon heating the sample, although some residual contribution is observed even after heating at room temperature.

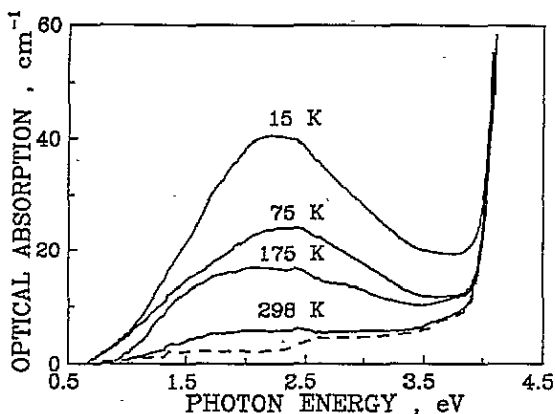


Figure 4. Optical absorption of  $MgNb_2O_6$  oxidized single crystals before x-ray irradiation (---), immediately after x-ray irradiation for 15 h at 15 K (labelled 15 K) and after further heating for 10 min at the temperature indicated on each curve (labelled 75 K, 175 K and 298 K, respectively). All absorption spectra were measured at 15 K.

It is worth noting that the rates of annealing of this optical absorption are slightly different in the infrared and visible regions. In particular the spectrum observed after heating at 175 K shows the presence of a component close to 1.5 eV. Therefore this absorption is complex and must be considered as the convolution of several components.

### 3.3. Thermal reduction treatments and optical bleaching

The blue colouration exhibited by as-grown samples may be recovered by heating the samples in vacuum; however, some differences in the optical absorption arise. In order to induce the reduction, rather high temperatures (above 900°C) are required.

Figure 1 includes a comparison of the optical absorption spectrum of as-grown samples and those obtained after a vacuum reduction of previously oxidized  $MgNb_2O_6$  samples.

The most obvious difference between as-grown and reduced samples observed in figure 1 is that the intensity of the absorption in the ultraviolet region (about 3.5 eV) is larger in reduced samples than in the as-grown samples. Moreover reduced samples also show more intense absorption in the infrared (at 1.0 eV) although the relative intensity of this band depends on the time of reduction and the particular sample used. These differences lead us to conclude that reduced samples contain more types of defect than as-grown samples do.

As will be discussed in section 4, some of the contributions to the optical absorption spectra arise from the presence of polaron centres. The absorption of these centres shows dichroism [16]. Figure 5(a) shows the optical absorption measured at 15 K for light polarized parallel to the  $C_3$  axis of the oxygen octahedron (i.e. parallel to the [001] axis of the  $MgNb_2O_6$  lattice) and perpendicular to it (i.e. parallel to the [100] axis of the lattice).

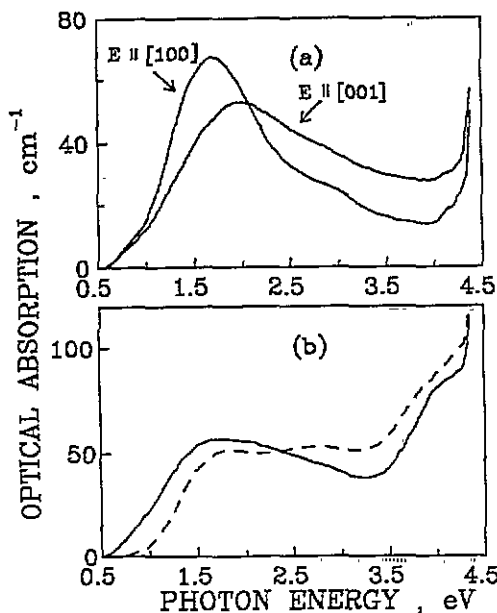


Figure 5. (a) Polarized optical absorption of as-grown  $\text{MgNb}_2\text{O}_6$  single crystals measured at 15 K. The curves are labelled with the light polarization directions. (b) Influence of the low-temperature (77 K) illumination on the optical absorption of a  $\text{MgNb}_2\text{O}_6$  crystal reduced in vacuum ( $10^{-2}$  mbar) for 3 d: ---, before illumination; —, illumination for 20 min with 351 nm laser light ( $300 \text{ mW cm}^{-2}$ ). The optical absorption has been measured at 77 K.

These spectra show a well resolved contribution at around 1.7 eV. Moreover, a minor component around 1.0 eV is also observed, as well as other unresolved contributions for energies higher than 2.5 eV.

In addition to these features, the thermal reduction induces a decrease in the pre-edge absorption observed after oxidation annealing in air.

The spectral distribution of the optical absorption of reduced crystals can be modified if the sample is illuminated at a low temperature (77 K) with ultraviolet light; we call this optical bleaching. Figure 5(b) shows the optical absorption spectrum recorded at 15 K of a reduced sample before and after illumination with the 351 nm (3.53 eV) line of an  $\text{Ar}^+$  laser.

As a result of the illumination the optical absorption for photon energies higher than 2.5 eV decreases and a parallel increase in the 0.5–2.0 eV region is observed. These changes are reversible on heating the sample to room temperature. This effect may be observed even with visible light, 514 nm (2.41 eV), but the efficiency of the bleaching is very low.

#### 4. Discussion

Figure 1 shows that by heating  $\text{MgNb}_2\text{O}_6$  in air the sample becomes transparent; therefore the colouration observed in as-grown and reduced samples is most probably due to the loss of oxygen from the lattice. This is likely to happen during crystal growth because of the very high temperature required for growth (about  $1620^\circ\text{C}$ ) and the low oxygen partial pressure of the growth atmosphere.

Well oxidized samples show a good transparency over the infrared and visible regions but in figures 1–3 we have shown that this treatment induces some absorption below the band edge. This pre-edge absorption gives rise to an emission at a low energy (2.5 eV). The photoluminescence of niobium oxides is generally understood as arising from the de-excitation of ionic clusters involving  $\text{Nb}^{5+}$  ions [17–19]. Therefore most probably the

pre-edge absorption and the weak emission associated with it are due to the presence of a small amount of Nb ions in an environment different from that corresponding to the regular Nb position. In fact, ceramic  $MgNb_2O_6$  samples, in which disorder may be expected to be larger than in single crystals, show an intense absorption tail from the absorption edge to below 3.0 eV [20].

X-ray irradiation at low temperatures and thermal reduction in vacuum induce colouration (see figures 1, 4 and 5(b)). All these spectra keep some common features with the optical absorption observed in as-grown samples.

Figure 5(a) shows clearly that the optical absorption of as-grown samples is dominated by a component at 1.69 eV. This band looks similar to the 1.6 eV band ascribed in  $LiNbO_3$  to  $Nb^{4+}$  small polarons (i.e. one electron trapped in an isolated  $Nb^{5+}$  ion) [21]. In addition to the optical absorption ascribed to  $Nb^{4+}$  polarons, other contributions at about 1.0 eV and above 2.5 eV may be observed in figure 5(a).

X-ray irradiation produces the excitation of electrons and holes which remain trapped at a sufficiently low temperature. Holes are most probably trapped in oxygen ions bound to a defect charged negatively with respect to the lattice (e.g. a Mg vacancy). This produces an  $O^-$ -bound small polaron. Electrons are most probably trapped at cations. Thus the optical absorption ascribed previously to  $Nb^{4+}$  must contribute to the absorption displayed in figure 4 after x-ray irradiation. In  $LiNbO_3$  doped with Mg an electron trap absorbing at 1.03 eV has been found [22]. Because of the similarity between the spectral position of this absorption and that found in  $MgNb_2O_6$  at 1.2 eV, we propose that the latter is due to a Mg-related electron trap centre.

In order to describe the optical absorption observed after x-ray irradiation, we have performed a phenomenological fit of the absorption assuming Gaussian bands for the optical absorption of Mg-related electron traps and  $Nb^{4+}$  polarons and fitting the rest of the spectrum with Gaussian contributions.

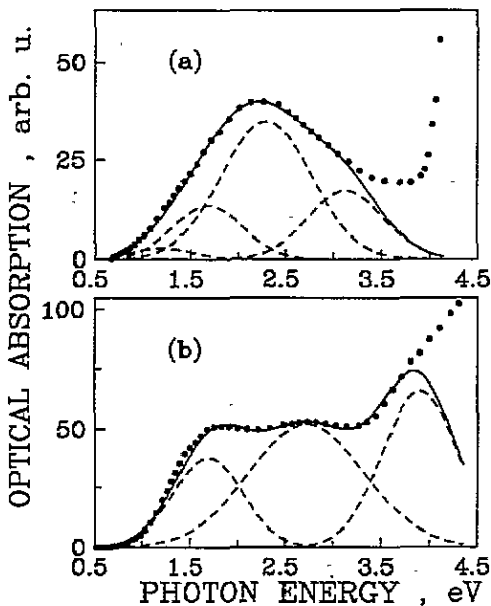


Figure 6. Gaussian decomposition of the optical absorption measured at 15 K of  $MgNb_2O_6$  single crystals. (a) Absorption induced by 15 K x-ray irradiation. (b) Absorption induced by thermal reduction in vacuum ( $1 \times 10^{-2}$  mbar) for 3 d at 970 °C: ●, experimental values of the absorption; ---, Gaussian bands used in the fitting; —, convolution of the Gaussians. The parameters of the Gaussians used are summarized in table 1.

The result has been plotted in figure 6(a) and is summarized in table 1. The most intense band observed at 2.30 eV is similar to that found in  $LiNbO_3$  after x-ray irradiation under



Table 1. Centre energy position  $E_0$  and band width  $\Delta E$  of the Gaussian contributions used for fitting the 15 K optical absorption of  $\text{MgNb}_2\text{O}_6$  and  $\text{LiNbO}_3$  after x-ray irradiation (XR) and thermal reduction in vacuum (RED).

$\text{MgNb}_2\text{O}_6$		$\text{LiNbO}_3$		Comments
$E_0$ (eV)	$\Delta E$ (eV)	$E_0$ (eV)	$\Delta E$ (eV)	
1.20	0.75	1.03 <sup>a</sup>	0.79	Mg-related electron traps; XR-RED
1.69	0.85	1.60	0.78	$\text{Nb}^{4+}$ polarons; XR-RED
2.30	1.10	2.50	1.66	$\text{O}^-$ -bound polarons; XR
3.13	0.92	3.22	0.60	Origin uncertain; XR
2.72	1.40	2.6	1.58	Nb bipolarons; RED
3.90	0.91	3.2	0.58	Origin uncertain; RED

<sup>a</sup> Observed in  $\text{LiNbO}_3:\text{Mg}$ .

similar experimental conditions [8] and its decrease upon heating to room temperature is basically parallel to the decrease in the absorptions associated with trapped electrons (1.20 and 1.69 eV). Therefore, it must be associated with trapped holes. The origin of the component at the high energy of 3.13 eV remains uncertain.

Reduced samples show an optical absorption that includes the bands observed in as-grown samples but further contributions appear. First the intensity in the infrared associated with Mg-related electron traps and  $\text{Nb}^{4+}$  polarons is comparatively larger in reduced samples than in as-grown samples. Secondly the contribution in the ultraviolet is much stronger in reduced samples. In figure 6(b) we show a possible decomposition in Gaussian components of the optical absorption of reduced samples. The parameters of the Gaussian bands used in the fit have been summarized in table 1.

Figure 5(b) shows that the electronic population of the different traps present in reduced samples may be redistributed by illumination at a low temperature. The bands at 2.72 and 3.90 eV decrease and enhance the absorption corresponding to electron traps (i.e.  $\text{Nb}^{4+}$  polaron and Mg-related traps). Therefore we conclude that the absorptions observed at 2.72 and 3.9 eV correspond to more complex electronic traps which are emptied by the light. This behaviour is qualitatively similar to that observed for  $\text{LiNbO}_3$  [5] although in our case the magnitude of the changes is smaller.

The origin of the band observed in  $\text{LiNbO}_3$  equivalent to our 2.72 eV band is a matter of controversy. Some workers attribute this band to the presence of F-type centres (electrons trapped in oxygen vacancies) [5, 6] while others assign this band to the presence of bipolarons (two electrons in neighbouring niobium ions) [3, 21]. *A priori*, both types of centre may be formed in  $\text{MgNb}_2\text{O}_6$ . We have seen that single electrons left after the oxygen loss are trapped at Nb ions (1.69 eV band). This shows that, irrespective of whether oxygen vacancies are being formed, Nb cations are very efficient traps for electrons and the formation of bipolarons seems likely.

In  $\text{MgNb}_2\text{O}_6$ , one would expect bipolarons to appear stochastically after a high degree of reduction of the sample. Our experimental results show that the ratio of the intensities of the 1.69 and 2.72 eV bands is quite independent of the reduction degree (see figure 1), which suggests that bipolarons are formed from the beginning of the reduction treatment. The following possibilities may be advanced to explain this behaviour.

- The formation of bipolarons on regular niobium ions is energetically favoured.
- Interstitial or Mg-antisited  $\text{Nb}^{5+}$  ions (both positively charged with regard to the lattice) are present and play an active role in electron trapping, giving rise to bipolarons.

The latter assumption is supported by the decrease in the pre-edge optical absorption observed in oxidized samples, which is ascribed to  $Nb^{5+}$  ions in environments different from the regular environment for Nb. The decrease in this absorption upon thermal reduction agrees with the annealing of  $Nb^{5+}$  ions sited at interstitial or Mg lattice sites after they trap an electron. Further work is required to confirm some of these models.

In conclusion we have shown that  $MgNb_2O_6$  crystals submitted to x-ray irradiation and vacuum reduction treatments exhibit optical absorption bands which may be compared with those observed in  $LiNbO_3$  after similar treatments. In view of this correlation,  $MgNb_2O_6$  may be considered as a reference for the discussion of the defects induced in  $LiNbO_3$ .

## Acknowledgments

The authors acknowledge the cooperation agreement between the Consejo Superior de Investigaciones Científicas (Spain) and the Hungarian Academy of Sciences (Hungary). The work has been partially supported by CICYT (Spain) under project MAT93-0095 and by the Scientific Research Foundation of Hungary under projects OTKA-14026 and OTKA-4241. The technical assistance of A Cintas (Madrid) with sample preparation is acknowledged.

## References

- [1] Armenise M N, Canali C, de Sarrío M and Zanoni E 1983 *Mater. Chem. Phys.* **9** 267
- [2] Krätzig E and Schirmer O F 1988 *Photorefractive Materials and their Application (Springer Topics in Applied Physics 61)* (Berlin: Springer) ch 5
- [3] Schürmer O F, Thiemann O and Wöhlecke M 1991 *J. Phys. Chem. Solids* **52** 185
- [4] Földvári I, Polgár K and Mecseki A 1984 *Acta Phys. Hung.* **55** 321
- [5] Sweeney K L and Halliburton L E 1983 *Appl. Phys. Lett.* **43** 336
- [6] Hodgson E R and Agulló-López F 1988 *Solid State Commun.* **64** 965
- [7] Carruthers J R, Kaminov I P and Stulz L W 1974 *Appl. Optics* **13** 2333
- [8] García-Cabañes, Sanz-García J A, Cabrera J M, Agulló-López F, Zaldo C, Pareja R, Polgár K, Raksányi K and Földvári I 1988 *Phys. Rev. B* **37** 6085
- [9] Pareja R, Gonzalez R and Pedrosa M A 1984 *Phys. Status Solidi a* **84** 179
- [10] Emmenegger F P and Roetschi H 1971 *J. Phys. Chem. Solids* **32** 787
- [11] Abrahams S C and Marsh P 1986 *Acta Crystallogr. B* **42** 61
- [12] Zaldo C, Gill D S, Eason R W, Mendiola J and Chandler P J 1994 *Appl. Phys. Lett.* **62** 502
- [13] Polgár K, Péter A, Paitz J and Zaldo C 1995 *J. Cryst. Growth* at press
- [14] Urbach F 1953 *Phys. Rev.* **92** 1324
- [15] Blasse G, Dirksen G J and Brixner L H 1986 *Mater. Chem. Phys.* **14** 485
- [16] Schirmer O F 1980 *J. Physique Coll.* **41** C6 479
- [17] Blasse G 1968 *J. Chem. Phys.* **48** 3108
- [18] Krol D M, Blasse G and Powell R C 1980 *J. Chem. Phys.* **73** 163
- [19] Zaldo C, Günter P and Arend H 1987 *Cryst. Latt. Def. Amorph. Mater.* **15** 123
- [20] Wachtel A 1964 *J. Electrochem. Soc.* **111** 534
- [21] Schirmer O F and von der Linde D 1978 *Appl. Phys. Lett.* **33** 35
- [22] Sweeney K L, Halliburton L E, Bryan D A, Rice R R and Tomaschke H E 1985 *J. Appl. Phys.* **57** 1036
- [23] Dutt D A, Feigl F J and De Leo G G 1990 *J. Phys. Chem. Solids* **51** 407